VHF radar and MF/HF dynasonde observations during Polar Mesosphere Summer Echoes conditions at EISCAT

Jann-Yenq Liu[1,2], Chen-Jeih Pan[1], and Chien-Chih Lee[1]

[1]*Institute of Space Science, National Central University, Chung-Li 32054, Taiwan*
[2]*Center for Space and Remote Sensing Research, National Central University, Chung-Li 32054, Taiwan*

The EISCAT VHF radar (224 MHz) and the EISCAT dynasonde (1–10 MHz) were operated simultaneously during a Polar Mesosphere Summer Echoes (PMSE) event on 22 June 1994. We investigate the echo characteristics revealed by these two instruments. The antenna of the VHF radar was set 10° off-zenith to the north for both transmission and receiving, while the dynasonde was operated with vertical beam to record ionograms every 3 minutes. The Height-Time-Intensity (HTI) variation of the VHF radar PMSE is studied, which is characterized layered structures. The intensity profiles are quite intermittent which show similarity to those data recorded by the dynasonde. To study the ionospheric condition with the dynasonde, the quantities of signal-to-noise ratio, echo frequency, echo polarization, echolocation, and Doppler velocity are investigated. Variations in the quantities demonstrate that during the PMSE conditions, echoes of the dynasonde are mainly attributed by reflection of many small irregularities within the observed ionospheric volume.

1. Introduction

The mesosphere is a particular difficult region of the atmosphere to be observed. In addition to sounding rockets and remote sensing by satellites, powerful radars on the ground are most appropriate to investigate this region. The discovery of remarkably strong echoes from the summer mesopause at VHF band has led to a pronounced interest in radio scattering from the mesosphere. These Polar Mesosphere Summer Echoes (PMSE), were first observed using the 50 MHz VHF radar at Poker Flat, Alaska (Ecklund and Balsley, 1981) but have subsequently been detected using a number of different radio sounding frequencies including 1.29 GHz, 933 MHz, 224 MHz, 53.5 MHz, and 8 MHz (for detail see, Cho and Kelley, 1993; Röttger, 1994; Cho and Röttger, 1997; Lee *et al.*, 2001, respectively). While Hoppe *et al.* (1990) found no correlation between PMSE and partial reflections at 2.78 MHz, Röttger (1994) reported about observations of PMSE at Tromsø (69°N, 19°E) on 224 MHz and simultaneous partial reflection at Murmansk (69°N, 36°E) on 2.7 MHz. Recently, Bremer *et al.* (1996) observed the simultaneous PMSE by the ALOMAR SOUSY radar at Andenes at 53.5 MHz, the EISCAT VHF radar at Tromsø at 224 MHz, and the MF radar at Tromsø at 2.78 MHz, which confirmed that the PMSE could be detected by MF and/or HF radars. To further understand the ionospheric quantities probed by MF/HF bands during the PMSE condition, we investigate signals from the mesosphere and lower thermosphere observed by the EISCAT VHF radar as well as the dynasonde at Tromsø on 22 June 1994.

2. Experimental Set-Up and Observation

Both the VHF radar and the dynasonde are collocated at the EISCAT Ramfjordmoen site (69°N, 19°E). On 22 June 1994, while the VHF radar was operated at 224 MHz, the dynasonde was operated in ionogram mode sweeping frequencies 1–10 MHz.

The EISCAT VHF radar antenna is a parabolic cylinder extending over 120 m in the zonal direction and 40 m in the meridional direction. During current experiment, the transmission was at 1 MW peak power through the eastern half of the antenna (60 m × 40 m) and this half as well as the western half were used for receiving in two channels. The half power beam width for each receiving antenna is about 1.2° in zonal direction. The antenna beams were pointing 10° off-zenith northward for both transmitting and receiving during the observation period. Detailed descriptions of the configurations of the EISCAT VHF radar can be found in La Hoz *et al.* (1989). A 64-baud complementary code with a 300 m range resolution was employed in this experiment. Samples at 29 range gates were coherently integrated over 29.85 ms; and 64 of these data points were collected in one record every 2 seconds. The altitude coverage was 81.45 km to 90.15 km, covering about the range where PMSE occurred most frequently (Czechowsky *et al.*, 1989; Cho and Kelley, 1993).

The dynasonde consists of a high power pulse transmitter and a pair of receiver channels. The installation of EISCAT dynasonde is considered to be optimum, which provides broad, uniform, nearly frequency and azimuthally-independent 'all-sky' illumination (Wright and Pitteway, 1994) with a vertex-down 2-plane log-periodic transmitting antenna. A square array of four or six receiving dipoles (Pitteway and Wright, 1992) near ground is receptive to echoes over a vertically directed similar wide angular range.
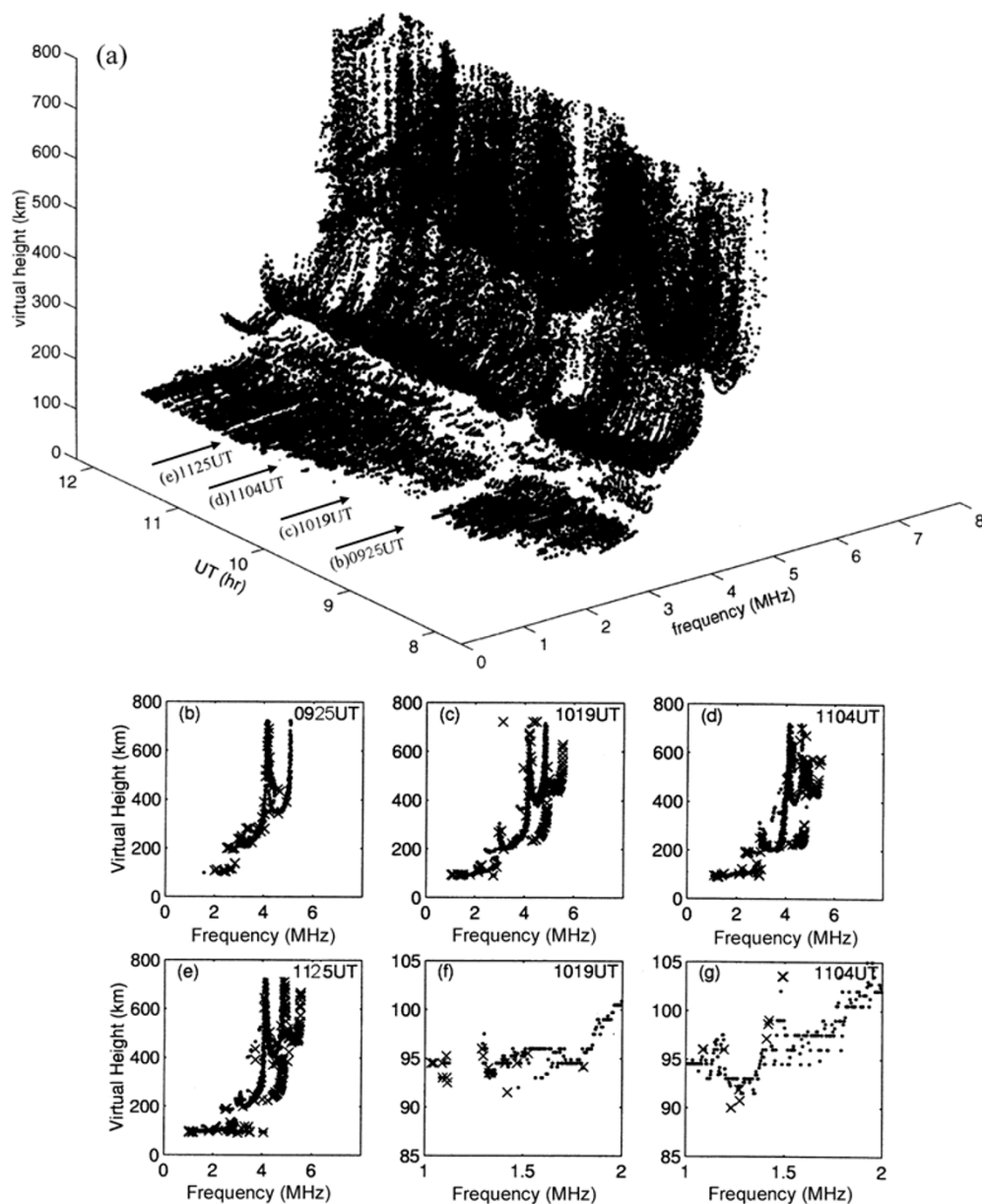
Fig. 1. Ionograms recorded by the EISCAT dynasonde during 0746–1200 UT 22 June 1994. (a) The ordinary (O-wave) component of the sequence of ionograms. Four typical ionograms at (b) 0925, (c) 1019, (d) 1104, and (e) 1125 UT. Magnified ionogram traces in lower ionosphere at (f) 1019, (g) 1104 UT. Dotted and cross symbols respectively denote the O- and X-wave components.

During this experiment, the high power transmitter was on, the transmission was at a peak power of 5 kW and the dynasonde derives ionograms every 3 minutes (Wright and Pitteway, 1979). Combining measurements obtained from the array of receiving antenna, we derive the parameters (or quantities) of echo amplitude, signal-to-noise ratio (SNR), echo polarization, echolocation, and Doppler velocity from the ionogram records (Pitteway and Wright, 1992; Tsai *et al.*, 1993).

3.   Results and Interpretations

During 0746–1200 UT (LT = UT+1 hour), 22 June 1994, a sequence of ionograms was recorded by the dynasonde. Figure 1(a) illustrates behavior of the ordinary (O-wave) component of the ionograms. We identify certain features of echoes on 1–4 MHz from below 100 km on the ionogram

records, which are presumed to be related to PMSE observed on 224 MHz with the VHF radar (see Fig. 2). Figures 1(b)–(e) show four typical ionograms recorded at 0925, 1019, 1104, and 1125 UT. Besides the normal echo traces from the F1 and F2 layer, we recognize the E-layer clearly. The F-region and E-region echoes reveal the ionosphere under a geomagnetic quiet condition ($Kp < 3-$), indicating also generally low D-region absorption, since echoes were observed as low as 1 MHz, except of at 0925 UT (see Fig. 1(b)) when a weak absorption event occurred (characterized by lowest observable frequency increase to 2 MHz and absence of the extra-ordinary (X-wave, cross symbols) component in the F1 and F2 layer echoes). After 1125 UT, a short-lasting sporadic E-layer (Es) with critical frequency of 4 MHz was observed (see Fig. 1(e)). It can be found that the normal E-layer critical frequency was around 3.5 MHz above 100 km
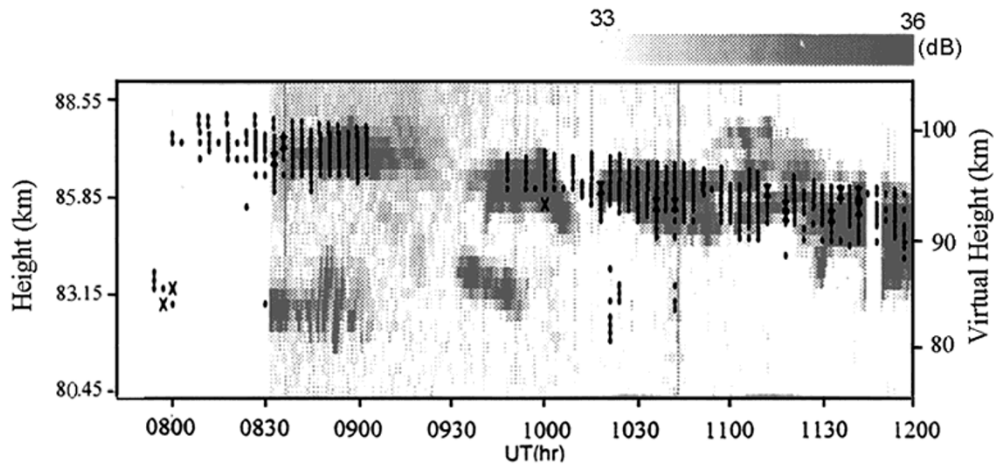
Fig. 2. The altitude versus time distribution of PMSE observed by the EISCAT VHF radar and the dynasonde. The gray level with the left vertical axis represents the returned power recorded by the VHF radar. The dot and cross with the right vertical axis are the ordinary- (O-) and extra-ordinary- (X-) mode echoes received by the dynasonde, respectively.

(Figs. 1(b)–(e)) while the lower E-region/upper D-region is at an altitude of about 90 km with critical frequencies 1–1.5 MHz (Figs. 1(f) and (g)). Figures 1(f) and (g), which are magnified from Figs. 1(c) and (d), show that there is no echo caused by strong derivative absorptions at about 1.2 MHz, and abrupt increase in virtual height due to the ledge (electron density valley or biteout) retardations at 1.2–1.4 MHz, respectively. These indicate that there are some sub-layers and/or electron density fluctuations in the D-region. Figure 2 shows the Height-Time-Intensity (HTI) plot of PMSE observed by the VHF radar (gray level) and echoes below about 100 km virtual height recorded by the dynasonde (dot and cross symbols). The intensity (echo power) of the VHF radar is presented in dB units, where 33 dB corresponds to the noise level. There is a data gap between 1145 and 1150 UT due to the radar transmission stop. We recognize five typical PMSE (two twin-layer and three single-layer) features, intermittently appearing between 82 to 87 km altitudes. The occurring is varying with height and time, which is characterizing a downward trend. From 0830 to 1010 UT, the two twin-layer, upper/lower, structures centered at 87.0/83.0 and 85.7/83.2 km altitude are present, respectively. The descent rate for the upper layer is about 1.5 km/h while the ascent rate for the lower layer is about 0.2 km/h. After 1010 UT, the three single-layer structures are noticed, and echo power of the one between 1050 and 1130 UT is slightly weaker than those of the other two. The descent rate of the single-layer structures is about 1.5 km/h. Note that, since the intermittent structures are detected 10° off-zenith, the echoes are mainly from a scattering dominant mechanism.

It is required that a certain electron density exists in the altitude of the PMSE in order to enhance the scatter cross section at this frequency, regardless of the principle scattering mechanism (Hocking, 1985). Since the abrupt increases in virtual height due to electron density biteouts appearing in Figs. 1(f) and (g), we, thus, attempted to compare the 224 MHz PMSE observations with the MF/HF dynasonde records below about 100 km virtual range. We recognize

from Fig. 2 that the upper PMSE layers of the VHF radar and the echoes of the dynasonde correlate between 0830 and 0903 UT and about 0945 and 1200 UT. However, portions of the PMSE layers seen by the VHF radar between 0906 and 0942 UT were not clear detected by the dynasonde. We consider the discrepancy is caused by the weak absorption event, which is manifest by the ionogram taken at 0925 UT (see, Fig. 1(b)). This absorption event is due to the enhanced D-region electron density. This in turn increases the signal power of PMSE, as noticed in the HTI plot of the VHF radar returned (Czechowsky *et al.*, 1989). On the other hand, the lower PMSE layers during 0830–0900 UT and 0930–0950 UT seen by the VHF radar were not observed by the dynasonde. This might result from electron density below 85 km altitude being too low, less than 1.0 MHz, to be detected by the dynasonde.

Figure 2 displays that during 0800–1200 UT the lowest (or bottom) of virtual height is descending from 98 to 90 km with a decent rate of about 1.8 km/h, which agrees with the downward trend with a decent rate 1.5 km/h of VHF PMSE appearing in the HTI plot. It is found that altitudes of bottom side of the intermittent features of the VHF radar are about 5–10 km lower than those of the dynasonde. Based on the two descent rates and bottom side altitudes, a downgoing upper bound at 100 and 95 km virtual heights is respectively adopted at 0830 and 1200 UT to examine the dynasonde data in further detail.

Using the VHF PMSE features shown in Fig. 2 as a reference background (gray level), Fig. 3 illustrates that various dynasonde parameters (ionospheric quantities) recorded below the upper bound. Figure 3(a) illustrates that SNR of the dynasonde generally has greater values when the VHF radar detects stronger intensities. Radiowave (or Plasma) frequencies of the intermittent features in Fig. 3(b) can be subdivided into two intervals that are 1.0–2.0 MHz (0800–1200 UT), and 2.5–3.0 MHz (1015–1200 UT). Multi-plasma frequencies simultaneously appearing at a certain altitude suggests that the ionosphere is not plane stratified but filled up with numerous irregularities. Figure 3(c) shows that the
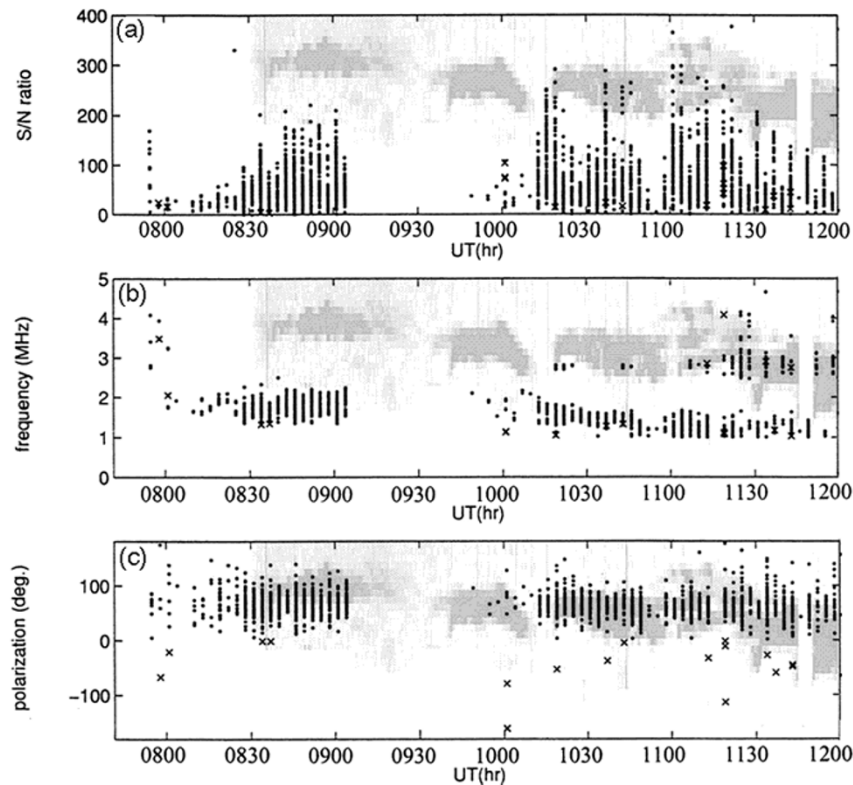
Fig. 3. Measurements obtained from the dynasonde (a) signal-to-noise ratio, (b) plasma frequency, (c) polarization, (d) NS range, (e) EW range, and (f) Doppler velocity. Dotted and cross symbols respectively denote the O- and X-wave components. The gray level is the HTI of the VHF radar as same as Fig. 2.

polarization of the echoes is corresponding to the O-wave component of the reflected wave. For the echolocations, Figs. 2, 3(d), and 3(e) reveal that when the VHF radar SNR increases, the reflection altitude of virtual height tend to be lower and the echo ranges in the north-south (NS) and east-west (EW) distances tend to be broader. It is clear from dynasonde sky maps that echo locations with PMSE conditions shown in Figs. 4(a) and (b) (respectively corresponding to Figs. 1(f) and (g) recorded at 1019 and 1104 UT) are more scattered than those without PMSE conditions shown by Figs. 4(c) and (d) (recorded at 1010 and 1016 UT). Both echolocations and skymaps indicate the irregularities act as targets that reflected and scatter the signals transmitted by the dynasonde. Finally, it can be found in Fig. 3(f) that the line-of-sight Doppler velocities in both away and toward directions, which generally lie between 200 and −200 m/s (−100 and +100 m/s) during 0830–0910 UT (1000–1200 UT), simultaneously increase. It is, thus, assumed that there were no large-scale irregularities or gradients of electron density causing scattering or partial reflection at the PMSE altitudes.

4. Discussions

Simultaneous observations with the EISCAT VHF radar and dynasonde were carried out during the PMSE observation on 22 June 1994. Five clear PMSE signatures were found in echo power of VHF radar during 0830 and 1200 UT, 22 June 1994. It is found that during 0830–0905 and 1010–1200 UT, the variations in ionospheric quantities de-

rived from the dynasonde agree well with the intermittent features of PMSE observed by the VHF radar. The discrepancies between the two measurements occurring during 0930–1010 UT and after 1125 UT could result from that the ionospheric absorption and the Es-layer during the PMSE observation of the MF/HF dynasonde soundings.

It is found from Fig. 2 that in the bottom side of echoing layer of the dynasonde is about 5–10 km higher than that of the PMSE upper layer of the VHF radar. The difference altitude could be caused by the retardation of the underly ionizations and/or the ledge effect (Lee *et al.*, 2000). Since the altitude of a PMSE is low, the associated electron density and underly ionization retardation are generally small and negligible. Budden (1985) and Titheridge (1985) based on the ray trace theory show that the virtual heights near a ledge (or valley/biteout), where the electron density gradient in upward direction is about zero (or changes from positive to negative values), could significantly increase. The abruptly increasing in virtual heights around 1.2–1.4 MHz illustrated in Figs. 1(f) and (g) indicate that there are biteouts and fluctuations in ionospheric electron density during the 22 June 1994 PMSE observation. Meanwhile, it might be the biteouts and/or the fluctuations, which result the bottom of the echo layer of the dynasonde being constantly about 5–10 km higher than that of the PMSE layer of the VHF radar. Note that the signatures of deep electron density biteouts (or ledges) as well as fluctuations of electron density in simultaneous MST radar and three rockets measurements during the PMSE condition are also reported by Ulwick *et*
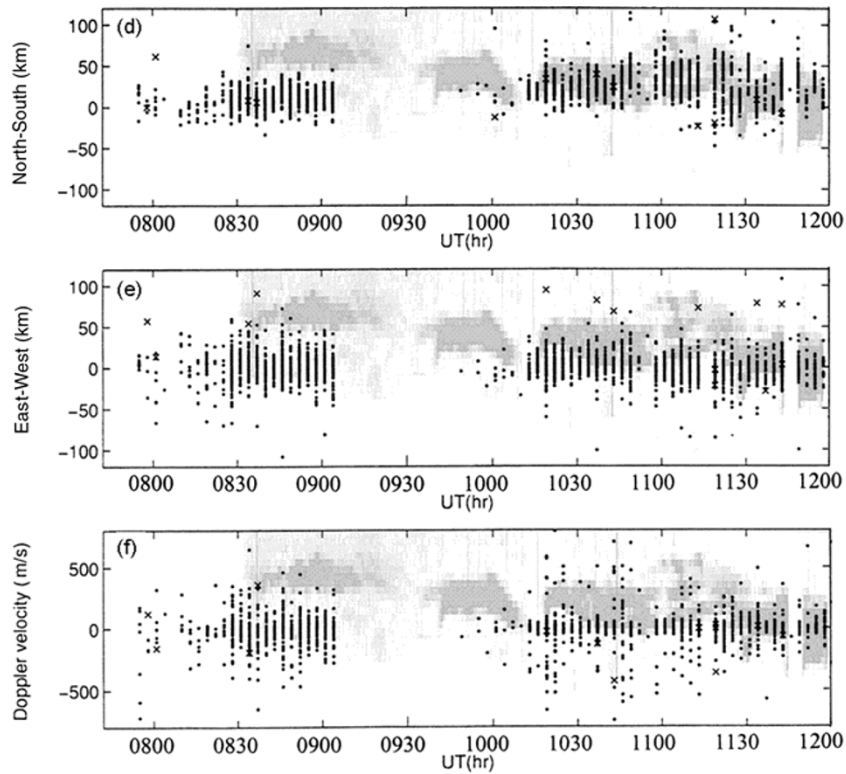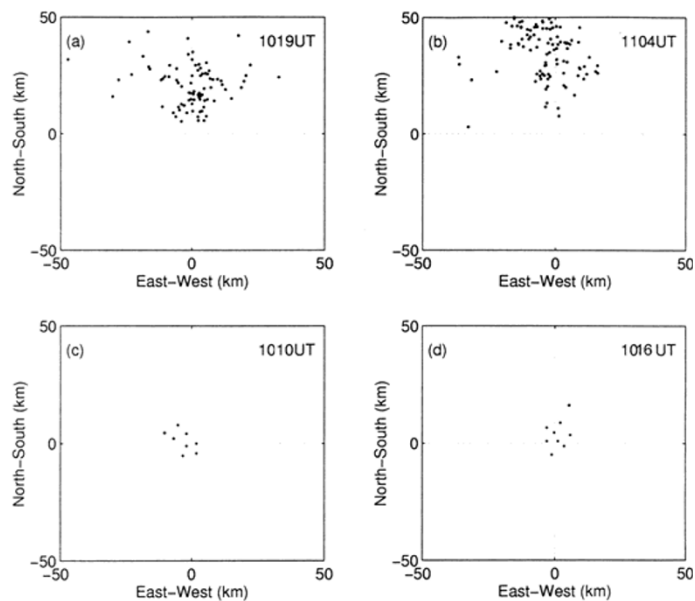
Fig. 3. (continued).

Fig. 4. The sky maps of echo location recorded at (a) 1019 UT and (b) 1104 UT with PMSE conditions, and (c) 1010 UT and (d) 1016 UT without PMSE conditions by the dynasonde.

al. (1988).

Figure 2 shows that above about 85 km altitude the observations of the VHF radar well agrees with those of the dynasonde, but there were almost no dynasonde echoes recorded below 85 km. It has been reported by many sounding rocket experiments (see Lübken *et al.*, 1998) that the electron density below 85 km is about 3000 el/cm^3 (about 0.5 MHz).

Note that 0.5 MHz is less than the sounding frequencies 1–10 MHz of the dynasonde. Therefore, we suggest that no echo returned from the lower PMSE layer is due to the low electron density that became unable to reflect the radio waves transmitted by the dynasonde.

It is well accepted by radio scientists that a distinct and isolated layer has steady values in its associated physical pa-
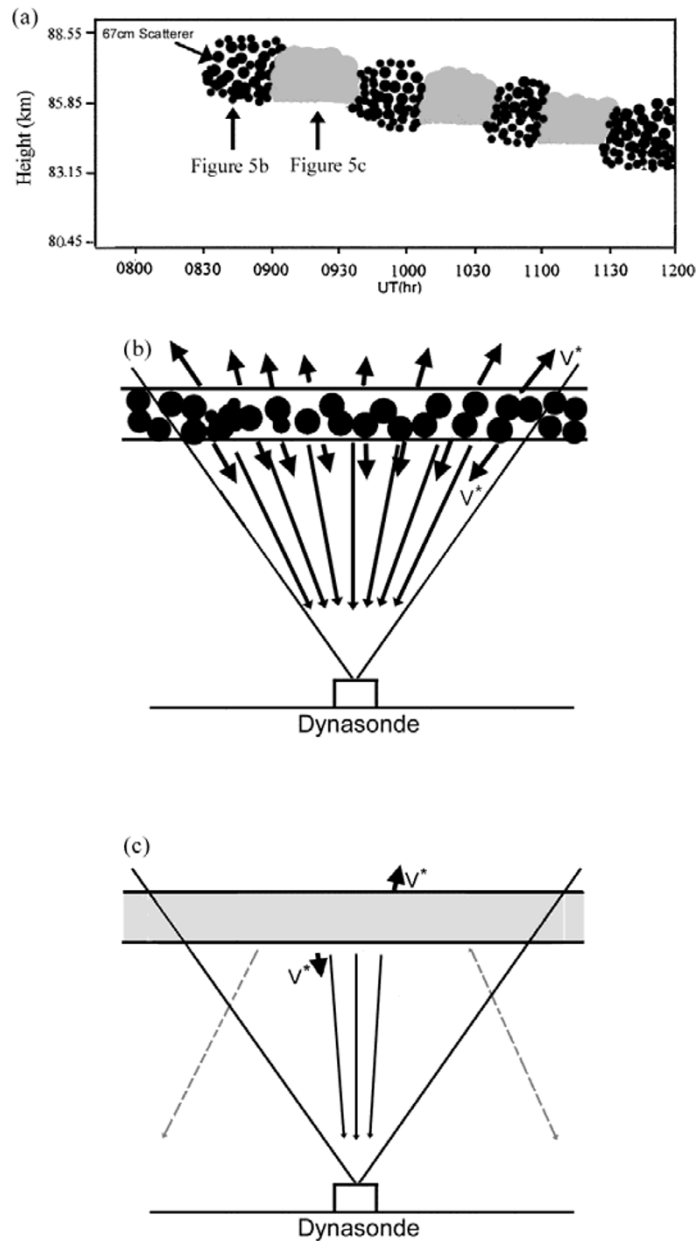
Fig. 5. (a) A sketch of the ionospheric electron density of Fig. 2. Antenna beam configurations (b) with and (c) without the PMSE. The thick vectors V*
    denote the Doppler velocities, and the dark arrow lines represent the numbers and directions of echo returns.

rameters, and a steady structure in its reflection altitude and horizontal ranges, while many small irregularities within the observed ionospheric volume result in the parameter fluctuations. Figure 5(a) is a sketch of the ionospheric density structure of Fig. 2, where the dots and patches denote the ionospheric electron density with and without small irregularities, respectively. Figs. 5(b) and (c) further simulates the dynasonde echoes under the two ionospheric conditions. It can be been the summation if the numerous small irregularities within the dynasonde radar volume results in a greater SNR (or echo power), broader NS/EW echolocations and larger Doppler velocity, V*, fluctuations observed (Fig. 5(b)). By contrast, a plane stratified density layer due to a small reflection area, the SNR, locations, and Doppler velocity fluctuation yield smaller values (Fig. 5(c)).

The PMSE effects have been detected by sounding fre-

quencies varying from 2.78 to 944 MHz and the possible scattering mechanisms, ranging from partial diffusion reflection to Thomson scatter (Cho and Röttger, 1997). The use of the dynasonde further extends the sounding frequencies as low as 1 MHz. To investigate the echo mechanism of dynasonde, we plot the echo counts at various echo amplitudes and plasma frequencies. Figure 6 shows that numerous echoes are observed around frequency 1.2 MHz; and echo counts and SNR at frequencies 1.0–1.75 MHz are much greater and stronger than those at 1.75–4.0 MHz. We further suggest that stronger echoes result from the total reflection from numerous small irregularities, while the weaker echoes are possibly caused by the partial reflections and/or scatterings of them. On the basis of the reflection mechanism, the ambient plasma frequency in this PMSE event is possibly as great as 1.75 MHz, which is about a factor of two of 0.8
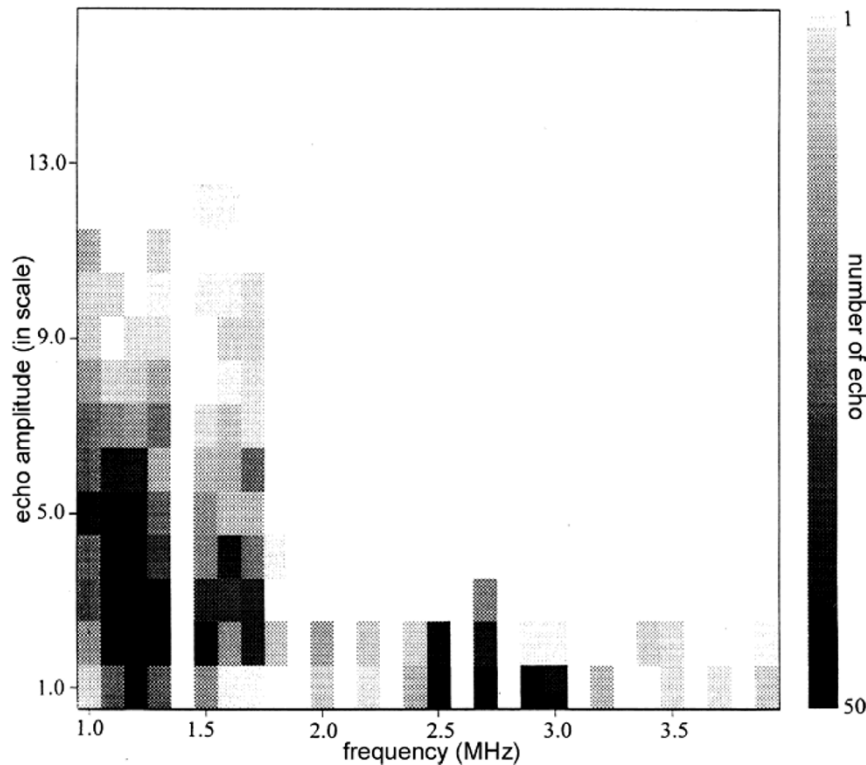
Fig. 6. Echo count for various echo amplitude and radiowave frequencies.

MHz reported by the previous rocket observation (Ulwick *et al.*, 1988).

5. Conclusions

The UHF (Thomson scattering), VHF (scattering), and MF (partial reflection) have been applied on the PMSE investigation in the early studies. This examination is the pioneer of presenting the PMSE signatures via the total reflection by using an ionosonde (dynasonde). In conclusions, we show that a MH/HF dynasonde (or ionosonde) can be employed to monitor ionospheric quantities during PMSE conditions. The abrupt increases in virtual heights of the dynasonde, and the altitude difference between EISCAT VHF radar and dynasonde suggest the coexistence of the bite-outs and fluctuations of ionospheric electron density around the PMSE layer. The intermittently enhanced SNR, multiplasma frequencies, scattered echolocation, and broadened Doppler velocity observed by the dynasonde demonstrate numerous small irregularities appearing during the PMSE conditions.

References

Bremer, J., P. Hoffmann, A. H. Manson, C. E. Meek, R. Ruster, and W. Singer, PMSE observations at three different frequencies in Northern Europe during summer 1994, *Ann. Geophysicae*, **14**, 1317–1327, 1996.

Budden, K. G., The propagation of radio waves, Cambridge University Press, 1985.

Cho, J. Y. N. and M. C. Kelley, Polar mesosphere summer radar echoes: observations and current theories, *Rev. Geophys.*, **31**, 243–365, 1993.

Cho, J. Y. N. and J. Röttger, An updated review of polar mesosphere summer echoes: Observation, theory, and their relationship to noctilucent clouds and subvisible aerosols, *J. Geophys. Res.*, **102**, 2001–2020, 1997.

Czechowsky, P., I. M. Reid, R. Ruster, and G. Schmidt, VHF radar echoes observed in the summer and winter polar mesosphere over Andfya, Norway, *J. Geophys. Res.*, **94**, 5199–5271, 1989.

Ecklund, W. L. and B. B. Balsley, Long-term observations of the Arctic mesosphere with the MST radar Poker Flat, Alaska, *J. Geophys. Res.*, **86**, 7775–7780, 1981.

Hocking, W. K., Measurement of turbulent energy dissipation rates in the middle atmosphere by radar techniques: A review, *Radio Sci.*, **20**, 1403–1422, 1985.

La Hoz, C., J. Röttger, M. Rietveld, G. Wannberg, and S. J. Frank, The status and planned developments of EISCAT in mesosphere and D-region experiments, *Middle Atmos. Program Hanbd.*, **28**, 476–488, 1989.

Lee, C. C., J. Y. Liu, C. J. Pan, and K. Igarashi, The heights of sporadic-E layer simultaneously observed by the VHF radar and ionosondes in Chung-Li, *Geophys. Res. Lett.*, **27**, 641–644, 2000.

Lee, C. C., J. Y. Liu, C. J. Pan, and C. H. Liu, Doppler velocities obtained by the EISCAT VHF radar and the dynasonde during the PMSE95 campaign, *J. Atmos. Solar Terr. Phys.*, **63**, 193–199, 2001.

Lübken, F. J., M. Rapp, T. Blix, and E. Thrane, Microphysical and turbulent measurements of the Schmidt number in the vicinity of polar mesosphere summer echoes, *Geophy. Res. Lett.*, **25**, 893–896, 1998.

Pitteway, M. L. V. and J. W. Wright, Toward and optimum receiving array and pulse set for the Dynasonde, *Radio Sci.*, **27**, 481–490, 1992.

Röttger, J., Polar mesosphere summer echoes: dynamics and aeronomy on the mesosphere, *Adv. Space Res.*, **14**, (9)123–(9)137, 1994.

Titheridge, J. E., Ionogram Analysis with the Generalized Program PLOAN, Rep. UAG-93, World Data Center A for Solar Terr. Phys., 1985.

Tsai, L.-C., F. T. Berkey, and G. S. Stiles, On the derivation of an improved parameter configuration for the Dynasonde, *Radio Sci.*, **28**, 785–793, 1993.

Ulwick, J. C., K. D. Baker, M. C. Kelly, B. B. Balsley, and W. L. Ecklund,

Comparison of simultaneous MST radar and electron density probe measurements during STATE, *J. Geophys. Res.*, **93**, 6989–7000, 1988.

Wright, J. W. and M. L. V. Pitteway, Real-time data acquisition and interpretation capabilities of the Dynasonde 1. Data acquisition and real-time display, *Radio Sci.*, **14**(5), 815–825, 1979.

Wright, J. W. and M. L. V. Pitteway, High-resolution vector velocity determinations from the dynasonde, *J. Atmos. Terr. Phys.*, **56**, 961–977, 1994.

J.-Y. Liu (e-mail: jyliu@jupiter.ss.ncu.edu.tw), C.-J. Pan, and C.-C. Lee